[11] C. Goldsbury, J. Kistler, U. Aebi, T. Arvinte, G. J. S. Cooper, *J. Mol. Biol.* **1999**, *285*, 33.
[12] B. Bohrmann, M. Adrian, J. Dubochet, P. Kuner, F. Müller, W. Huber, C. Nordstedt, H. Döbeli, *J. Struct. Biol.* **2000**, *130*, 232.
[13] H. Rapaport, K. Kjaer, T. R. Jensen, L. Leiserowitz, D. A. Tirrell, *J. Am. Chem. Soc.* **2000**, *122*, 12523.
[14] S. Matile, *Chem. Soc. Rev.* **2001**, *30*, 158.
[15] S. Matile, *Chem. Rec.* **2001**, *1*, 162.
[16] B. Baumeister, N. Sakai, S. Matile, unpublished results.
[17] B. Baumeister, A. Som, G. Das, N. Sakai, S. Matile, unpublished results.
[18] A. Engel, D. J. Müller, *Nat. Struct. Biol.* **2000**, *7*, 715.
[19] M. Adrian, J. Dubochet, S. D. Fuller, J. R. Harris, *Micron* **1998**, *29*, 145.

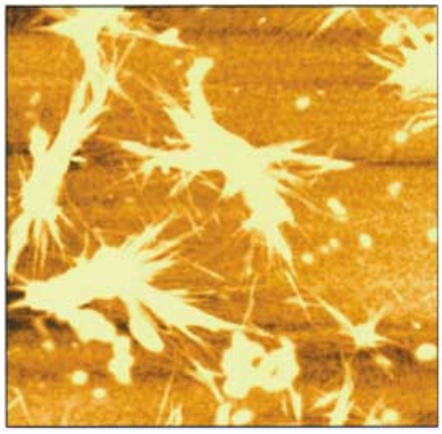

Figure 1. AFM image (5×5 μm) of carbon nanotube stars on mica. The reaction mixture was directly cast on mica without any purification.

Construction of Carbon Nanotube "Stars" with Dendrimers

Masahito Sano,* Ayumi Kamino, and Seiji Shinkai

Since carbon nanotubes are either metallic or semiconducting and exhibit ballistic transport,[1] the positioning of individual nanotubes in a well-defined spatial orientation may produce novel physical properties. By the currently available growth methods, carbon nanotubes are produced only in a stringlike form. Chemical modification is an attractive method for constructing various large-scale structures by positioning stringlike nanotubes. Herein we report the construction of star-shaped structures in which many carbon nanotubes radiate from a dendrimer center. These super-structured carbon nanotubes exhibit a peculiar response to electron beams. The synthesis of the stars was made possible by carefully fractionating the nanotubes by size.

Commercially available single-walled carbon nanotubes (SWNTs) are very long and are difficult to disperse in solution.[2–6] A standard procedure is to apply ultrasonication in strong acids to cut SWNTs into short pieces,[7, 8] followed by light etching to introduce oxygen-containing groups, such as carboxylic acids. Cut SWNTs are fractionated according to their characteristic sizes, as discussed herein. The carboxylic acid groups of the fractionated SWNTs were converted into acid chlorides and were then treated with the tenth generation poly(amidoamine) (PAMAM) starburst dendrimer (G10).

Atomic force microscopy (AFM) on cast films of the reaction mixture on mica reveals star-shaped objects (Figure 1). The average spine length is approximately 0.8 μm, which agrees well with the length of the SWNTs in the fraction. Although acid treatment tends to produce oxygen-containing groups at the side walls as well as at the ends,[9] our findings indicate, as proposed by other studies,[8, 10, 11] that the acid chloride groups at the open ends are more reactive than those at the side walls. Many spines are thicker than several nm and indicates, therefore, that there must be bundles of SWNTs in some burs. We think that many SWNTs simply adhere by van der Waals interactions to those tubes that have reacted with a dendrimer because of local high concentrations of tubes around the dendrimer. Some SWNTs are seen to bridge between two stars, which suggests that both ends of some SWNTs have reacted. Spectroscopic characterization was not possible because of the extremely low molar concentrations of stars that resulted from the initial low concentrations of SWNTs and difficulties in purification. Support that the SWNTs are covalently linked to the dendrimers rather than self-coagulated is provided by the observation that the star structures were completely destroyed after heating the stars for 3 h at 500 °C in N_2.

When the same sample shown in the AFM image of Figure 1 was coated with Pt/Pd and observed by scanning electron microscopy (SEM), star-shaped objects with much thicker burs were imaged. These spines were thicker than would be expected from the mere presence of the Pt/Pd films (Figure 2). Since the number of spines in the SEM image is smaller than that in the AFM image, it is likely that some of the spines in a star adhere together during residual water evaporation and metal deposition when they are placed in a vacuum. Without any metal coating, the acid-treated SWNTs

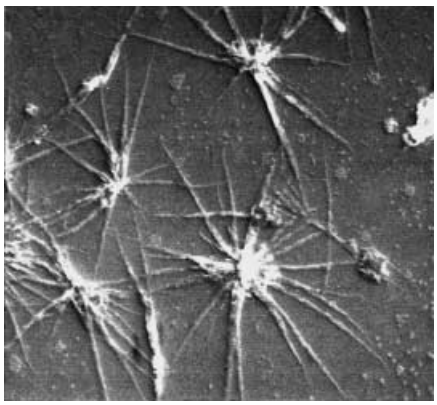

Figure 2. SEM image of the same sample as used to obtain Figure 1, but coated with Pt/Pd.

[*] Dr. M. Sano, A. Kamino, Prof. Dr. S. Shinkai
Chemotransfiguration Project—JST
2432 Aikawa, Kurume, Fukuoka 839-0861 (Japan)
Fax: (+81) 942-39-9012
E-mail: mass@jst.ktarn.or.jp

  1433-7851/01/4024-4661 $ 17.50+.50/0

that are not used for reaction usually give bright contrast on silicon surfaces when examined by SEM. Interestingly, some stars appear very dark when uncoated stars are imaged with the acid-treated SWNTs (Figure 3). It is not clear if all the stars give dark contrast since the acid-treated SWNTs form a network and hide the stars. While the mechanism is not well understood, the SEM results suggest that the star-shaped SWNTs may possess novel response characteristics to incoming electrons.

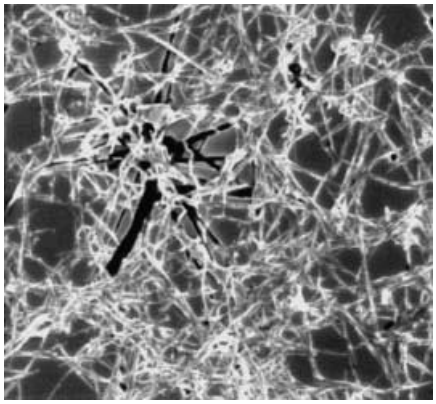

Figure 3. SEM image of a mixture of stars and the acid-treated SWNTs on silicon without any metal coating.

Cutting pristine SWNTs by acid produces SWNTs with a broad size distribution.[8] No star-shaped structures were recognizable by AFM or SEM when the whole distribution was used for the reaction with the dendrimers. This result can be rationalized by the reactivity of the SWNTs being size-dependent. If the number of oxygen-containing groups at both ends of a SWNT is independent of the tube length but the length affects the collision probability of the ends to other reactants, then chemical reactivity is expected to vary with the size of the SWNTs. Dynamic light scattering (DLS) was measured on various fractions collected at different centrifugal forces to ascertain the effect of size on the transport properties of SWNTs.[12] Here, a fraction collected as a supernatant solution with a centrifugal acceleration of G (in a unit of g) is designated G. Figure 4a plots the first cumulant Γ divided by the square of the wave number q as a function of G. In the case of a solid sphere, the initial relaxation rate Γ/q^2 is a translational diffusion constant. The stringlike shape of SWNTs, a broad length distribution within each fraction, and possible bundle formation, however, do not allow simple interpretation of Γ/q^2. Nevertheless, the value of Γ/q^2 reflects the structures and transport properties of SWNTs. The curve shows two regions of increasing Γ/q^2 values (at $G < 3500$ and $G > 12500$) and a plateau region between them. The scattering intensity was 5 to 10 times smaller at $G = 35300$ than for all other fractions.

AFM observations were also made on selected fractions from each region. All the samples show tubular and globular morphology. The measured length (for tubular moieties) or diameter (for globular moieties) exhibit histograms with a peak and a slowly decaying tail to larger sizes. The peak positions are depicted in Figure 4b. The higher the G value is,

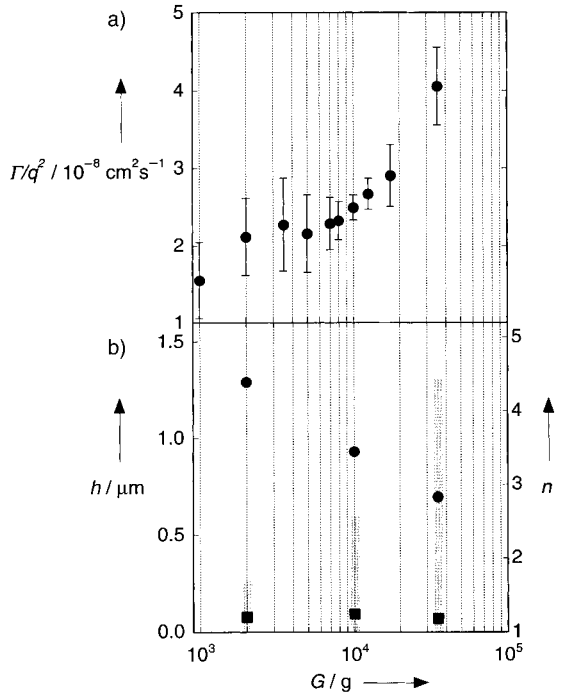

Figure 4. a) A plot of the initial relaxation rates Γ/q^2 obtained by DLS measurements against the centrifugal acceleration G used to fractionate the SWNTs dispersion. b) The most abundant length (circles) and diameter (squares) of the tubular and globular aggregates, respectively, at selected fractions. The vertical bars indicate the ratio of globular aggregates to tubular aggregates found in the AFM images. h = size, n = ratio of globular to tubular aggregates.

the shorter the tubular aggregates become. The globular aggregates have the same size regardless of the G value, but are found more in the higher G fractions. Globular morphology is considered to result from the aggregation of very short tubes during solvent evaporation.

We have shown previously that a SWNT has a persistence length of 0.8 μm.[13] Since this value agrees well with the tube length in the plateau region, the first increase of Γ/q^2 at $G <$ 3500 is most likely caused by a change in tube conformation. Those SWNTs in the region $G > 3500$ are stiff and straight, whereas SWNTs at smaller G values are semiflexible. Although physical factors that cause the second increase of Γ/q^2 at $G > 12500$ are not well understood, the higher G fractions contain larger numbers of very short SWNTs that move faster. The stars, as shown above, were obtained by using only those SWNTs in the plateau region. When the higher G fractions were added, the AFM images appear indistinguishable from those of physical mixtures without reaction. This result suggests that very short tubes reacted with the dendrimers before the longer ones had chance to do so. This study demonstrates the importance of size control for the construction of well-defined nanotube objects.

Experimental Section

SWNTs (a laser-oven product purchased from Tubes@Rice with an average radius of 0.6 nm) were cut by ultrasonication in strong acids and lightly etched in H_2SO_4/H_2O_2,[7, 8] followed by washing on a teflon filter with water until the filtrate became neutral. The SWNTs were dispersed in solvents by ultrasonication for 60 s in a laboratory ultrasonic washing bath (42 kHz,

  1433-7851/01/4024-4662 $ 17.50+.50/0

90 W). Water was used for the DLS measurement and DMF for the reaction. The SWNT dispersion was subjected to a series of centrifugations starting from the largest force. Each time, a supernatant solution was separated from the heavier residue, which was redispersed for further centrifugation. The concentration of each supernatant solution was adjusted to 1.0 $\mu g\,mL^{-1}$. DLS measurements were performed with a wavelength of 632.8 nm and a scattering angle of 90° at 30 °C and the data were analyzed with a cumulant method. Measurements have been repeated several times using different batches of the acid treatments. Subsequent experiments showed that the measurements were performed on SWNTs in the concentration-independent region.

The SWNT fractions in the plateau region were treated with thionyl chloride to produce SWNTs derivatized with acid chloride groups, as reported by others.[8, 10] In the present case, we used centrifugation and decantation cycles to wash the acid chloride-derivitized SWNTs with dry THF and DMF to minimize coagulation. A dispersion of acid chloride-derivatized SWNTs in DMF (10 μL) was added to the dendrimer (G10) dissolved in 10 mM NaOH. The concentration of SWNTs was so low that the solution hardly had any color. This was necessary, since amine-terminated dendrimers act as a glue to stick SWNTs together and coagulate the SWNTs immediately.[14] The mixture was stirred at room temperature for 12 h and the reaction mixture was directly cast on mica or silicon for AFM and SEM studies.

AFM was performed in a noncontact mode in air at room temperature. SEM images were taken with an acceleration voltage of 5.0 kV for Pt/Pd coated samples and 1.0 kV for uncoated samples.

Received: August 13, 2001 [Z17718]

[1] R. Saito, G. Dresselhaus, M. S. Dresselhaus, *Physical Properties of Carbon Nanotubes*, Imperial College, London, **1998**.

[2] P. J. Boul, J. Liu, E. T. Mickelson, C. B. Huffman, L. M. Ericson, I. W. Chiang, K. A. Smith, D. T. Colbert, R. H. Hauge, J. L. Margrave, R. E. Smalley, *Chem. Phys. Lett.* **1999**, *310*, 367 – 372.

[3] B. Z. Tang, H. Xu, *Macromolecules* **1999**, *32*, 2569 – 2576.

[4] K. D. Ausman, R. Piner, O. Lourie, R. S. Ruoff, M. Korobov, *J. Phys. Chem. B* **2000**, *104*, 8911 – 8915.

[5] J. L. Bahr, E. T. Mickelson, M. J. Bronikowski, R. E. Smalley, J. M. Tour, *Chem. Commun.* **2001**, 193 – 194.

[6] A. Star, J. F. Stoddart, D. Stueuerman, M. Diehl, A. Boukai, E. W. Wong, X. Yang, S.-W. Chung, H. Choi, J. R. Heath, *Angew. Chem.* **2001**, *113*, 1771 – 1775; *Angew. Chem. Int. Ed.* **2001**, *40*, 1721 – 1725.

[7] A. G. Rinzler, J. Liu, H. Dai, P. Nikolaev, C. B. Huffman, F. J. Rodríguez-Macías, P. J. Boul, A. H. Lu, D. Heymann, D. T. Colbert, R. S. Lee, J. E. Fischer, A. M. Rao, P. C. Eklund, R. E. Smalley, *Appl. Phys. A* **1998**, *67*, 29 – 37.

[8] J. Liu, A. G. Rinzler, H. Dai, J. H. Hafner, R. K. Bradley, P. J. Boul, A. Lu, T. Iverson, K. Shelimov, C. B. Huffman, F. Rodriguez-Macias, Y.-S. Shon, T. R. Lee, D. T. Colbert, R. E. Smalley, *Science* **1998**, *280*, 1253 – 1256.

[9] D. B. Mawhinney, V. Naumenko, A. Kuznetsova, J. T. Yates, Jr., J. Liu, R. E. Smalley, *Chem. Phys. Lett.* **2000**, *324*, 213 – 216.

[10] J. Chen, M. A. Hamon, H. Hu, Y. Chen, A. M. Rao, P. C. Eklund, R. C. Haddon, *Science* **1998**, *282*, 95 – 98.

[11] Z. Liu, Z. Shen, T. Zhu, S. Hou, L. Ying, Z. Shi, Z. Gu, *Langmuir* **2000**, *16*, 3569 – 3573.

[12] Short SWNTs can be fractionated by chromatography: S. Niyogi, H. Hu, M. Hamon, P. Bhowmik, B. Zhao, S. M. Rozenzhak, J. Chen, M. E. Itkis, M. S. Meier, R. C. Haddon, *J. Am. Chem. Soc.* **2001**, *123*, 733 – 734.

[13] M. Sano, A. Kamino, J. Okamura, S. Shinkai, *Science* **2001**, *293*, 1299 – 1301.

[14] J. Liu, M. J. Casavant, M. Cox, D. A. Walters, P. Boul, W. Lu, A. J. Rimberg, K. A. Smith, D. T. Colbert, R. E. Smalley, *Chem. Phys. Lett.* **1999**, *303*, 125 – 129.

Direct Microscopic Observation of the Time Course of Single-Molecule DNA Restriction Reactions**

Bürk Schäfer, Helgard Gemeinhardt, and Karl Otto Greulich*

While biophysical studies, such as force measurements[1–4] or laser cutting[5] of single DNA molecules can be found in the literature in a large variety of applications, direct light-microscopic detection of DNA single molecule reactions is rare. In most of the latter cases, unstained DNA molecules were coupled to microspheres (beads) and held with optical or magnetic tweezers. The reaction was then observed indirectly by the change of some distance or force, for example, displacement of the sphere reflected the reaction progress.[6–10] In this sense, single DNA-molecule reactions are usually detected in "blind" experiments. One of the exceptions is the direct microscopic observation of the reaction of fluorescently stained *E.-coli*-RNA-polymerase on unstained DNA.[11] One particularly interesting class of reactions are those of restriction endonucleases, since they allow individual DNA molecules to be characterized and distinguished. As many as 3000 different restriction endonucleases of one subclass (type II) are known.[12] The observation of restriction reactions is, however, difficult, since the restriction step is an all-or-none process, that is, cut or non-cut, of the DNA molecule at a given restriction site. To date, single-molecule restriction has been observed by blind cutting of individual fluorescently marked DNA molecules and analyzing the fluorescence bursts of the restriction fragments.[13]

We have already reported the cutting of a single, bead-coupled DNA molecule by the restriction endonuclease Apa 1, which has one cutting site in the target molecule,[14] and the restriction by Sma I and Eco RI with three and five cutting sites.[15] Herein, we introduce temporal resolution and thus information on the kinetics of single DNA-molecule restriction.

Figure 1 shows the restriction of a single DNA molecule by the enzyme Eco RI. In part (g) of Figure 1, the cutting pattern expected from the 48502 base pairs (bp) long sequence of Lambda phage DNA is shown. The molecule is stretched by hydrodynamic flow from bottom right to top left. In the example shown the DNA end with the longest restriction fragment (21226 bp) is attached to the bead. Binding of the short fragment (3530 bp) is also observed, but then usually only one or two cuts can be detected since some restriction sites are in the part of the DNA molecule which is wrapped around the bead. Such wrapping causes the bead fluorescence seen in Figure 1.

At a given time, usually 5 – 20 seconds after injection of the enzyme, the first cut is seen (Figure 1b); this point is then

[*] Prof. Dr. K. O. Greulich, B. Schäfer, H. Gemeinhardt
Institut für Molekulare Biotechnologie
Postfach: 100 813, 07708 Jena (Germany)
Fax: (+49) 3641-656410
E-mail: kog@imb-jena.de

[**] We thank Dr. Werner Wolf for helpful discussions and the VW-foundation, Grant No. I/75099 for supporting this work.